Assessing vaccine-mediated protection in an ultra-low dose *Mycobacterium tuberculosis* murine model

*Plumlee, C.R.[1], *Barrett, H.W.[1,2], Shao, D.E.[3], Lien, K.A.[1], Cross, L.M.[1], Cohen, S.B.[1], Edlefsen, P.T[3], Urdahl, K.B.[1,4,5,6,†]

[1] Center for Global Infectious Disease Research, Seattle Children's Research Institute, Seattle, WA, 98109, USA

[2] University of Washington, Dept. of Global Health, Seattle, WA, 98109, USA

[3] Vaccine and Infectious Disease Division, Fred Hutch Cancer Center, Seattle, WA, 98109, USA

[4] University of Washington, Dept. of Immunology, Seattle, WA, 98109, USA

[5] University of Washington, Dept. of Pediatrics, Seattle, WA, 98109, USA

[6] Lead Contact

[†]Correspondence: Kevin.Urdahl@seattlechildrens.org

*Equal contributions

ABSTRACT

Despite widespread immunization with Bacille-Calmette-Guerin (BCG), the only currently licensed tuberculosis (TB) vaccine, TB remains a leading cause of mortality globally. There are many TB vaccine candidates in the developmental pipeline, but the lack of a robust animal model to assess vaccine efficacy has hindered our ability to prioritize candidates for human clinical trials. Here we use a murine ultra-low dose (ULD) *Mycobacterium tuberculosis* (Mtb) challenge model to assess protection conferred by BCG vaccination. We show that BCG confers a durable reduction in lung bacterial burdens, curbs Mtb dissemination to the contralateral lung, and prevents detectable infection in a small percentage of mice. These findings are consistent with the ability of human BCG vaccination to mediate protection, particularly against disseminated disease, in specific human populations and clinical settings. Overall, our findings demonstrate that the ultra-low dose Mtb infection model can measure distinct parameters of immune protection that cannot be assessed in conventional dose murine infection models and could provide an improved platform for TB vaccine testing.

53 **INTRODUCTION**

54 New and effective tuberculosis (TB) vaccines are urgently needed. Although BCG vaccination
55 can provide protection in infants and older children in some clinical settings[1-4], it has proven to
56 be inadequate to combat the global pandemic. There are numerous TB vaccine candidates in
57 the developmental pipeline[5], but it will not be feasible to conduct human efficacy trials for most
58 of them. The standard for assessing vaccine efficacy is prevention of disease, which occurs in
59 only a small percentage of infected individuals, resulting in dauting sample sizes and costs
60 needed to complete human trials. Unfortunately, identifying promising vaccine candidates to
61 prioritize for human efficacy trials has been hindered by the lack of reliable animal models that
62 adequately predict human TB vaccine efficacy[6,7].

63

64 Historically, mice have been the most commonly used model for testing TB vaccine candidates
65 due to their ease of use, cost-effectiveness, and the relative conservation of the mammalian
66 immune system. However, limitations in the current mouse model, in which mice are infected
67 with ~50-100 CFU by aerosol, have shaken confidence regarding how well findings in mice can
68 be translated to humans[6,7]. There is minimal variability in the performance of different vaccines
69 in the current model. Most TB vaccines confer ~1 log of protection, reducing the lung burden
70 from ~10^6 to ~10^5 CFU, but only if assessed 4-6 weeks after aerosol challenge. This protection
71 is transient and usually dissipates by 3-4 months post-infection (p.i.)[8,9]. Furthermore, it is
72 unclear if the vaccine-induced mechanisms that enable mice to transiently reduce their bacterial
73 burdens in the setting of an ultimately unsuccessful immune response are relevant to the types
74 of immunity required for long lasting protection against the clinical manifestations of human TB.
75 Because mice in this model are unable to eradicate, or even durably control Mtb, some have
76 suggested that mice may lack the fundamental immune effector molecules needed for Mtb
77 control[10]. The failure of mouse vaccine testing to reliably predict results in human TB vaccine

78 trials have reinforced these concerns about the relevance of the mouse model for TB vaccine
79 testing[6,7].
80

81 Recently we developed a physiologic ultra-low dose (ULD) (i.e., 1-3 CFUs) Mtb mouse infection
82 model that more closely resembles several aspects of human Mtb infection[11]. Here we test the
83 ability of the ULD challenge model to assess immunity conferred by BCG vaccination, the
84 vaccine for which the most human efficacy data exists. In contrast to the conventional dose
85 model, we show that BCG-vaccinated mice challenged with 1-3 Mtb CFU exhibit a more durable
86 reduction in lung bacterial burdens. Vaccinated mice had an increased ability to contain
87 infection to a single lung and prevent Mtb dissemination to the contralateral lung. Finally,
88 vaccinated mice exhibited a significantly higher proportion of animals with no detectable
89 infection. Thus, the ULD model provides a promising platform for TB vaccine testing, as it
90 affords the opportunity to measure distinct parameters of vaccine-mediated immunity that
91 cannot be assessed in the current mouse model.
92

93 **RESULTS**

94 **BCG-mediated reduction of lung bacterial burdens is transient in the current mouse**
95 **model.**

96 The capacity of BCG to mediate protection in C57BL/6 (B6) mice infected with 50-100 Mtb CFU
97 has been assessed by many labs, but we sought to repeat this experiment in our own hands to
98 directly compare the conventional dose with the ULD model. We subcutaneously immunized B6
99 mice with 10^6 BCG-Pasteur 8 weeks prior to aerosol challenge with H37Rv Mtb and determined
100 the lung bacterial burdens at days 42 and 120 post-infection. As previously shown[8,9], BCG
101 immunization provided about one log of protection against lung bacterial burden at day 42, but
102 this protection was transient and dissipated at later timepoints; there was no significant

103 difference in bacterial burdens between unimmunized and BCG-immunized mice at day 120
104 post-infection (**Figure 1)**.
105
106 **Measuring vaccine-mediated immunity in the ULD Mtb model.**
107 Next, we assessed the efficacy of BCG in the ULD aerosol Mtb challenge model, a model in
108 which the aerosolized dose is reduced with a goal of infecting only ~60-80% of the mice in the
109 infection chamber[11]. As previously described using an ULD infection of a pool of bar-coded Mtb
110 strains, the number founding strains detected using bar-codes after ULD infection approximates
111 a Poisson distribution; most mice are infected with a single founding Mtb strain, whereas fewer
112 are infected with two or three founding strains[11]. **Figure 2** depicts a BCG immunization
113 experiment in which we assessed the bacterial burdens in the right and left lungs separately and
114 in the spleen 9 weeks after aerosol ULD challenge. Amongst those mice with detectable
115 infection, we observed that, compared to unimmunized mice, BCG-immunized mice had lower
116 overall lung bacterial burdens (pooling right and left lungs) (**Figure 2A**), and lower spleen
117 bacterial burdens (**Figure 2B**). We also observed that 7/20 of the unimmunized mice and 10/20
118 of the BCG-immunized mice had no detectable infection in either lung (**Figure 2A**), a difference
119 that was not statistically significant in this single experiment (p=0.53). While the same seven
120 mice with undetectable lung bacterial burdens also had no detectable splenic bacterial burdens,
121 two mice that did have detectable lung infection in the BCG-immunized group failed to show
122 evidence of splenic bacterial burdens (12/20 BCG-immunized mice had no recoverable Mtb
123 from their spleen, compared to 10/20 from the lungs). Thus, BCG immunization appeared to
124 prevent splenic Mtb dissemination or promote splenic Mtb clearance.
125
126 To further assess the capacity of BCG immunization to restrict Mtb dissemination, we also
127 assessed bacterial burdens separately in the right and left lungs. In the ULD model, since
128 infection is usually established by a single founding Mtb strain, the lungs are often colonized

129 unilaterally; most commonly, the right lung is colonized because the right lung and bronchus are
130 larger than the left[11]. Our previous ULD studies using bar-coded Mtb strains showed that
131 bilateral lung infection usually represents the dissemination of a single Mtb strain from the
132 infection-seeded lung to the contralateral lung. In the experiment shown in **Figure 2**, we
133 observed that 5/10 of the BCG-immunized mice exhibited unilateral lung infection compared to
134 only 1/13 of the infected unimmunized mice (p= 0.023; **Figure 2C and D**). Of the two BCG-
135 immunized mice with pulmonary Mtb infection but no detectable splenic bacterial burdens, one
136 was infected in the right lung only while the other had bilateral lung infection (**Figure 2D**). Thus,
137 the ULD model has the capacity to assess a vaccine's ability to prevent dissemination, a
138 parameter of protection that cannot be assessed in conventional dose infections because
139 dissemination occurs in all mice regardless of vaccination status.
140
141 **BCG confers durable reductions in lung bacterial burdens in ULD-challenged mice.**
142 As previously shown[8,9], and as demonstrated in **Figure 1**, BCG-mediated reductions in lung
143 bacterial burdens are abrogated by 100-120 days post-challenge. To assess the durability of
144 BCG-mediated protection in the ULD model, we performed a time course and assessed
145 bacterial burdens in the lungs and spleen of ULD-infected mice at an early (d14), intermediate
146 (d42), and late timepoint (d115). At day 14 post ULD-infection, bacterial burdens were similar in
147 both unimmunized and BCG-immunized infected mice, but at days 42 and 115, bacterial
148 burdens were reduced by approximately one log (p=0.002 and p<0.001 respectively; **Figure**
149 **3A**). These data suggest that BCG-mediated reductions of lung bacterial burdens are more
150 durable in ULD-infected mice compared to conventional dose-infected mice, but the intentional
151 heterogeneous nature of the model makes it difficult to draw conclusions based on a single
152 experiment.
153

154 Next, we performed multiple ULD challenge experiments comparing BCG immunized vs.
155 unimmunized mice to rigorously assess the reproducibility of our findings. **Supplemental Table**
156 **1** shows results from 31 individual experiments assessing BCG efficacy in the ULD model,
157 representing a total of 537 unimmunized and 543 BCG-immunized mice with lung bacterial
158 burdens assessed at timepoints ranging from days 14-125 post-infection. **Figure 3B** shows the
159 combined (right and left lungs pooled) bacterial burdens from all experiments binned by similar
160 timepoints post-infection. Similar to prior reports using a conventional dose Mtb challenge[12,13],
161 BCG had no effect on bacterial burdens at the earliest timepoints assessed, days 14-15 post-
162 infection. However, BCG-immunized mice had lower lung bacterial burdens than unimmunized
163 mice at every later timepoint. This reduction remained robust (~1 log) even at days 90-125 post-
164 infection. Thus, unlike the transient reduction of bacterial burdens observed in the conventional
165 dose Mtb challenge model[8,9], BCG durably reduces the lung bacterial burdens in ULD-
166 challenged mice for at least 4 months post-infection.
167
168 **BCG prevents Mtb dissemination to the contralateral lung.**
169 To better assess the reproducibility of BCG's capacity to prevent dissemination, we assessed
170 the proportion of mice with bilateral vs. unilateral lung infection in all experiments shown in
171 **Supplemental Table I**. Based on raw CFU data, there was no difference in the proportion of
172 mice with bilateral lung infection between unimmunized vs. BCG-immunized groups at days 14-
173 15 post-infection. At this early timepoint, the proportion of mice with bilateral lung infection was
174 low even in unimmunized mice, suggesting that dissemination had not yet occurred in either
175 group. This conclusion is supported by the observation that <20% of ULD-infected mice had
176 detectable splenic Mtb burdens at d14 post-infection (data not shown). At all later timepoints,
177 however, the proportion of mice with bilateral lung infection was higher in unimmunized
178 compared to BCG-immunized mice (**Figure 4A**). Although bilateral lung infection in the ULD
179 model usually reflects Mtb dissemination from the initially infected lung to the contralateral lung,

180 it can sometimes represent separate aerosolized infections by distinct bacilli in each individual
181 lung. To assess true dissemination more accurately, we ULD-infected mice with a pool of 50
182 bar-coded H37Rv Mtb strains that we have previously characterized[11]. Amplified genomic DNA
183 extracted from bacterial colonies of each infected mouse lung were sequenced to determine the
184 number of unique founding Mtb strains in each lung (**Figure 4B**). Because the probability of
185 separate infections with the same bar-coded strain is only ~1 in 78 when using the 50 bar-coded
186 Mtb pool in the ULD model[11], bilateral lung infection with a single Mtb strain in both lungs likely
187 represents true dissemination (e.g. BCG 36L and 36R). In contrast, when mice have different
188 Mtb strains in each lung (e.g. BCG 28L and 28R), this reflects separate infections of each lung.
189 Thus, if dissemination to the contralateral lung is assessed by bacterial burden alone without
190 assessing Mtb bar-codes, the ability of a vaccine to prevent dissemination will be
191 underestimated due to falsely categorizing separate infections in each lung as dissemination
192 events. In this experiment, BCG was deemed to have 50.2% efficacy ($p = 0.002$); **Figure 4C**) in
193 preventing dissemination when measured as the proportion of mice with bilateral Mtb infection.
194 However, if dissemination was defined as the proportion of mice that possessed at least one
195 identical bar-coded Mtb strain in both lungs, then BCG exhibited an efficacy of 73.5% ($p =$
196 0.001, **Figure 4D**). Compiling data from all experiments in which we performed bar-coded
197 infection and sequencing (n=5) revealed that BCG exhibited 79.7% efficacy in preventing
198 dissemination of Mtb to the contralateral lung ($p < 0.001$; **Figure 4E**).
199
200 **BCG immunization can prevent detectable infection.**
201 Finally, we compared the proportion of unimmunized and BCG-immunized mice that presented
202 with undetectable pulmonary infection. Pooling the data from all experiments assessed at D14-
203 15 after Mtb challenge (n=6), we observed no difference in the proportion of mice with
204 undetectable bacterial burdens in the BCG-immunized vs. unimmunized groups (**Figure 5A**).
205 However, at all later timepoints, we observed more mice with undetectable bacterial burdens in

206 BCG-immunized mice than in unimmunized mice. Excluding the six experiments assessed at
207 D14-15 when no difference was seen, we plotted the remaining 25 experiments at timepoints
208 from D26-125 as the proportion of mice with undetectable bacterial burdens in the unimmunized
209 vs. BCG-immunized group (**Figure 5B**). Although only three experiments (15-20
210 mice/group/experiment) reached statistical significance on their own (all in the BCG-immunized
211 group), most experiments (18 of 25) had a higher proportion of mice with undetectable bacterial
212 burdens in the BCG-immunized group. When the compiled data from all 25 of these
213 experiments were assessed (**Figure 5B**, black filled circle), the difference in the proportion of
214 mice with undetectable bacterial burdens in the BCG-immunized compared to the unimmunized
215 group was relatively modest (13% efficacy in preventing detectable infection), but highly
216 statistically significant ($p = 0.001$).
217
218 We also examined the number of founding strains in each mouse for all ULD experiments using
219 the pool of bar-coded strains (9 experiments with unimmunized mice and 6 with BCG-
220 immunized) (**Figure 5C**). As expected from the Poisson distribution, most unimmunized mice
221 were infected with only one strain, and fewer mice were infected with two or more strains. There
222 were similar proportions of unimmunized and BCG-immunized mice infected with two or more
223 Mtb strains. However, fewer BCG-immunized mice were infected with one founding Mtb strain
224 (36.9% of unimmunized mice versus 22.9% of BCG-immunized mice, $p = 0.011$), whereas more
225 BCG-immunized mice had zero Mtb strains (33.0% of unimmunized mice versus 48.3% of BCG-
226 immunized mice, $p = 0.008$). This suggests that infection attributable to a single founding Mtb
227 strain may be more readily prevented by BCG-mediated immunity than infection due to two or
228 more strains, but further investigation is needed to test this possibility more rigorously.
229
230 The demonstration that vaccine-induced immunity can prevent detectable Mtb infection in ULD-
231 infected mice opens the possibility of assessing a new and important immune parameter for TB

232 vaccine testing that was not known to be achievable in mice. However, BCG had a very low
233 capacity to mediate this type of protection (13% efficacy, p = 0.001); large numbers of mice
234 were required to reach statistical significance, which would not be practical for routine testing of
235 TB vaccine candidates. Because the overarching goal is to identify vaccines that are more
236 efficacious than BCG, we performed a power calculation to determine what level of vaccine
237 efficacy would be required to feasibly measure prevention of infection with a reasonable number
238 of mice (**Table 1)**. This analysis showed that a vaccine with 50-60% efficacy could be assessed
239 with a sample size of 28-55 mice per group, which would be achievable by pooling results from
240 2-3 experiments. Such a pipeline could be feasible, as Vidal et al. recently reported that a novel
241 live attenuated Mtb vaccine was dramatically more effective than BCG in the ULD challenge
242 model, and prevention of detectable infection could be measured in a statistically significant
243 manner with only 18 mice per group[25]. Taken together with our findings, these results suggest
244 that the ULD challenge model provides a larger window to measure differences between TB
245 vaccine candidates and to measure parameters of protection, including inhibition of
246 dissemination and prevention of detectable infection, that cannot be assessed in currently used
247 mouse models.
248
249 **DISCUSSION**
250 Despite widespread vaccination with BCG, TB remains a major cause of global morbidity and
251 mortality[14]. Although surpassed for a couple years by SARS-CoV-2 as the leading cause of
252 death due to a single infectious organism, recent mortality estimates for each infection suggest
253 that TB is again the number one cause of infectious death[14]. New vaccines that provide better
254 efficacy than BCG are needed. To triage the growing number of TB vaccine candidates and
255 move those with the most promise into clinical trials, there is an urgent need to develop small
256 animal models that reliably assess parameters of immunity with relevance to human protection.
257 There is growing concern that the current mouse model, in which mice are infected with 50-100

258 Mtb CFU by aerosolization, is not up to this task[6,7]. This model provides too small a window to
259 discern differences between vaccine candidates; most confer a transient reduction in the lung
260 bacterial burden by about one log if measured between 4-6 weeks post-infection. Durable
261 reductions in lung bacterial burdens and other clinically relevant parameters of immunity,
262 including the ability to curb Mtb dissemination or prevent detectable infection, are difficult or
263 impossible to assess. Indeed, the inability of the current model to predict how well vaccine
264 candidates will perform in human efficacy trials is becoming increasingly apparent[6,7]. In this
265 study, we demonstrate that the ULD murine model provides a promising new challenge model in
266 which three distinct parameters of protection can be assessed: 1) durable reductions in lung
267 bacterial burdens, 2) inhibition of Mtb dissemination, and 3) prevention of detectable infection.
268
269 Of these, reduction in bacterial burdens is the only parameter of protection that can readily be
270 assessed in current mouse models. In contrast to transient protection that dissipates within 3-4
271 months in the current model[8,9], we have shown durable lung bacterial burden reductions for at
272 least four months in the ULD model. Importantly, the types of immune responses that mediate
273 reductions in lung bacterial burdens in mice infected with high doses (>250 CFUs) are
274 sometimes different than those that do so at conventional doses (50–100 CFU)[15,16]. Although
275 this has not yet been rigorously assessed in the ULD model, it is reasonable to hypothesize that
276 the optimal immune responses that are optimal for reducing lung bacterial burdens after a
277 physiologic dose challenge of 1-3 CFU may also be different than those required for a 50-100
278 CFU challenge. Thus, vaccine candidates may vary in their capacity to control bacterial burdens
279 to a physiologically relevant challenge dose compared to a challenge dose that is artificially
280 high, a hypothesis that needs further investigation.
281
282 The second parameter of immunity that can be measured in the ULD model is the ability to
283 prevent dissemination. Because most ULD-infected mice are infected by a single founding

284 bacillus[11], infection is usually initiated at a single site in one lung. Thus, most bilateral lung
285 infection is the result of Mtb dissemination from the initially infected lung to the contralateral lung
286 and CFU determinations of each individual lung can provide an estimation of a vaccine's ability
287 to block dissemination, which we have termed containment. This approach underestimates
288 containment, however, because some mice may have Mtb in each lung not because of
289 dissemination, but due to independent infection events of each lung by two or more distinct
290 aerosolized strains. By infecting mice with a pool of bar-coded strains, we have shown that we
291 can distinguish between disseminated infection and separate infections with different strains by
292 sequencing the Mtb bar-codes in each lung. Using this approach, we have shown that BCG
293 immunization can prevent Mtb dissemination to the contralateral lung in ~80% of ULD-infected
294 mice. These results in the murine ULD model parallel results in BCG vaccinated humans
295 showing that BCG vaccination is most effective at preventing disseminated forms of TB[17].
296
297 The third parameter of immunity that can be assessed in the ULD model is the prevention of
298 detectable infection. There are several lines of evidence that the human immune system can
299 prevent or eradicate Mtb infection. Some individuals with high exposure to index cases with
300 active TB disease, including household contacts, fail to develop an Mtb-specific IFNγ-producing
301 T cell response, suggesting that long-term Mtb infection is sometimes not established despite
302 intense exposure[18]. Furthermore, many individuals that do develop a T cell IFNγ response
303 against Mtb may eventually eradicate infection, as the incidence of active TB is quite low
304 amongst IGRA+ individuals (usually less than 5%) even when their immune systems are
305 potently immunosuppressed or ablated[19]. Recently there have been several high-profile TB
306 vaccine studies showing that some vaccines can prevent detectable infection in non-human
307 primates[20-22]. This had not been previously shown in mice, and it has been postulated that mice
308 lack the fundamental immune effectors needed to prevent sustained Mtb infection[10]. In this

309 study we showed no difference in the proportion of BCG-immunized mice with detectable
310 infection compared to controls at d14-15 after Mtb challenge, suggesting that vaccination did not
311 block the initial Mtb infection. At all later timepoints, however, BCG vaccinated animals had a
312 modest, but highly statistically significant increase in the proportion of mice with undetectable
313 infection compared to unimmunized controls (overall 13% efficacy, p=0.001). This suggests that
314 a small proportion of the vaccinated mice that may have been initially infected were able to clear
315 Mtb to undetectable levels. Even though BCG can do this only modestly, these results suggest
316 that vaccine-mediated immunity can prevent sustained infection in mice exposed to a
317 physiologic Mtb dose, challenging the longstanding belief stemming from experiments with an
318 artificially high Mtb exposure dose, that mice are unable to eradicate Mtb infection.
319
320 One limitation of the ULD model for vaccine testing is the number of animals that are required in
321 each group. This is exacerbated by the fact that not all animals are initially infected in the model,
322 and currently it is not possible to discern animals that were never infected from those that were
323 initially infected, but subsequently eradicated Mtb. We have attempted to develop both
324 immunologic and molecular assays to distinguish between these possible outcomes, but this
325 has proven difficult to achieve. We initially assessed Mtb-specific CD4 T cell responses against
326 an Mtb antigen (ESAT-6) that is not present in BCG. We identified a couple unvaccinated mice
327 that were exposed to aerosolized ULD Mtb and had measurable Mtb ESAT-6-specific CD4 T
328 cell responses despite having no detectable lung bacterial burdens. These results suggested
329 that even a few unvaccinated ULD-infected mice may clear Mtb to undetectable levels, but mice
330 exhibiting this phenotype were rare. However, this approach was not successful in BCG-
331 immunized mice because BCG immunization suppressed the development of Mtb ESAT-6-
332 specific T cells to undetectable or almost undetectable levels even in ULD Mtb-challenged mice
333 that were demonstrably infected, providing minimal window to discern differences between
334 uninfected and infected mice. We also attempted to amplify Mtb DNA from lung homogenate

335 using previously published Mtb-specific PCR primers[23]. Unfortunately, the sensitivity of this
336 assay was not sufficient to reliably detect below 1,000 viable bacteria, and we were unable to
337 obtain a signal from mice with undetectable bacterial burdens. Despite our inability to
338 differentiate mice that were never infected from those who cleared infection, we were able to
339 build strong statistical evidence for prevention of detectable infection by assessing large
340 numbers of mice.
341
342 Our results are consistent with findings that BCG can sometimes provide long-term protection
343 against human TB, and are consistent with studies showing BCG-mediated protection in
344 individuals without prior Mtb exposure (tuberculin skin test-negative or IGRA-negative
345 individuals) or in low Mtb transmission settings[1-4]. The low overall observed efficacy (~13%) in
346 preventing detectable infection also reflects the suboptimal nature of BCG-mediated immunity.
347 Reliably assessing this parameter of protection for a vaccine with such low efficacy would
348 require hundreds of mice per group, as in this study, which would not be feasible for routine pre-
349 clinical evaluation of TB vaccine candidates. However, the goal is to identify promising vaccine
350 candidates that are significantly more efficacious than BCG to move into human trials. Our
351 power analysis showed that a vaccine with 50% efficacy could be readily assessed by repeating
352 studies with 15-20 mice per group 2-3 times and compiling the results. We believe this is
353 feasible and would be worthwhile if further studies show that results obtained in the ULD model
354 are superior to those obtained in the conventional murine model for distinguishing vaccine
355 efficacies in clinical meaningful ways. We are encouraged that a recent study assessing a novel
356 TB vaccine candidate (ΔLprG, a live-attenuated Mtb vaccine) in the ULD mouse model showed
357 that ΔLprG was dramatically better than BCG at preventing detectable infection and achieved
358 statistical significance with only 18 mice per group[25]. In this same study, ΔLprG was only slightly
359 better than BCG in reducing lung bacterial burdens in mice challenged with 100 CFU,

360 suggesting that the ULD challenge model provides a larger window to discriminate differences
361 between vaccines.
362
363 Overall, the ULD challenge model holds promise as a new and improved platform for evaluating
364 TB vaccine candidates. The model can assess distinct parameters of vaccine-mediated
365 immunity that cannot be assessed in the current mouse model and has potential to improve
366 discrimination between the protective capacities of different vaccines. Each of the three
367 parameters of immunity that can be assessed in the ULD model may be relevant to different
368 clinical TB outcomes. For example, the ability of vaccines to durably reduce lung bacterial
369 burdens and prevent dissemination may reflect their capacity to prevent different aspects of TB
370 disease, whereas the ability to prevent detectable infection may reflect prevention of sustained
371 infection. Because each of these parameters are likely mediated by different aspects of
372 immunity, it is possible that different vaccines will differ in the relative capacity to control Mtb
373 burdens, inhibit dissemination, and prevent detectable infection. Future studies are needed to
374 assess a variety of TB vaccine candidates in the ULD model, and whenever possible, determine
375 whether the results correlate with clinical outcomes in human vaccine trials.
376

377 **ACKNOWLEDGMENTS**

378 The authors would like to thank Bridget Alexander, Lindsay Engels, Samuel Schrader, Kaitlin
379 Durga and the Seattle Children's OAC staff for technical support. This work was supported by
380 NIH contract 75N93019C00070 (K.B.U), the Bill and Melinda Gates Foundation, INV-026296
381 (K.B.U) and NIH grant U19AI135976 (K.B.U).
382

383 **FIGURE LEGENDS**

384 **Figure 1. BCG-mediated reductions in Mtb lung burdens are not durable in a**
385 **conventional-dose infection.** C57BL/6 (B6) mice were aerosol infected with a conventional

386 dose (CD) (50-100 CFU) of H37Rv Mtb eight weeks following either subcutaneous (s.c.)
387 immunization with 10^6 BCG-Pasteur (BCG) or no immunization (unimmunized). On day 42 or
388 120 post-infection, CFU were enumerated from lung homogenates plated onto 7H10 plates.
389 These data represent 5 mice per group and are shown as mean ± SEM. Single-group
390 comparisons were analyzed using an unpaired t test. ***p<0.001.
391
392 **Figure 2. Assessing BCG efficacy in the ultra-low dose Mtb model.** B6 mice were aerosol
393 infected with an ULD (1-3 CFU) of H37Rv Mtb 8 weeks following either s.c. immunization with
394 10^6 BCG-Pasteur (n=20) or no immunization (n=20). On day 63 post-infection, CFU were
395 enumerated from left lung, right lung, or spleen homogenates plated onto 7H10 plates. **A)**
396 Combined lung CFUs or **B)** spleen CFUs from unimmunized and BCG-immunized mice are
397 graphed. Counts from left lungs, right lungs and spleen are graphed separately from, **C)**
398 unimmunized mice or **D)** BCG-immunized mice. There were 20 mice per group, and the data
399 are graphed as mean ± SD. Single-group comparisons were analyzed using an unpaired t test.
400 **p<0.01, ****p<0.0001.
401
402 **Figure 3. BCG-mediated reductions in Mtb lung burden are durable in the ULD model. A)**
403 Combined lung CFU from a single experiment time course of ULD-infected B6 mice with or
404 without BCG immunization. Combined lung CFU were enumerated on days 14, 42, and 115
405 post-infection. There were 19 or 20 mice per group, and the data are graphed as mean ± SD.
406 Single-group comparisons were analyzed using an unpaired t test. ***p<0.001, ****p<0.0001. **B)**
407 Combined lung CFU from a compilation of 31 experiments separated by timepoint post-infection
408 of ULD-infected B6 mice with or without BCG immunization. Error bars are 95% confidence
409 intervals in a fixed effects negative regression model. All timepoints except days 14-15 post-
410 infection have a p < 0.001.
411

412 **Figure 4. BCG-immunization prevents Mtb dissemination to the contralateral lung. A)**
413 Proportion of mice with bilateral lung infection (CFU in left and right lung) from a compilation of
414 31 experiments separated by timepoint post-infection of ULD-infected B6 mice with or without
415 BCG immunization. Error bars are 95% confidence intervals in a mixed effects logistic
416 regression model, with experiment as a grouping variable. All timepoints except days 14-15
417 post-infection have a $p \leq 0.001$. **B)** A single ULD experiment using bar-coded Mtb strains is
418 shown. On day 65 post-infection, right and left lung homogenates were plated onto 7H10 plates
419 and Mtb colonies from infected lungs were scraped to make genomic DNA. DNA was
420 sequenced, and the identity of each bar-coded Mtb strain is graphed for each lung separately.
421 The percentage of bilateral infection for unimmunized and BCG-immunized mice from this
422 experiment was calculated by the proportion of mice with CFUs in both lungs **(C)** or the
423 proportion of mice with at least one common Mtb strain in both lungs **(D)**. **(E)** The percentage of
424 mice with bilateral Mtb strains was compiled from 5 independent experiments, excluding day 14
425 post-infection. Vaccine efficacy for preventing dissemination to the contralateral lung was
426 calculated as 1-(% BCG mice with bilateral infection)/(% Unimmunized mice with bilateral
427 infection).
428
429 **Figure 5. BCG immunization prevents detectable infection in some mice. A)** Table of all
430 mice, showing the percentage with 0 CFU in the unimmunized vs BCG-immunized groups
431 separated by timepoint post-infection. **B)** The proportion of unimmunized mice with 0 CFU (x-
432 axis) vs the proportion of BCG-immunized mice with 0 CFU (y-axis) for each experiment from a
433 compilation of 25 experiments (days 26-125) separated by timepoint post-ULD infection. Each
434 colored symbol is an independent experiment, and the larger black circle is the compilation of all
435 the data, which was statistically significant (mixed effects logistic regression $p = 0.001$). Post-
436 hoc analyses indicated that, if each infection cohort had been analyzed separately, the 3 filled in
437 symbols would have attained statistical significance if they had been analyzed using the same

438 regression model ($p<0.05$), see supplemental Figure 1. **C)** In ULD-Mtb experiments in which
439 bar-coded strains were used for infection (n=9 for unimmunized, n=6 for BCG-immunized), the
440 mice are graphed according to the number of unique Mtb strains recovered from each mouse's
441 lungs.
442
443 **Table 1. Group sizes needed to assess vaccine-mediated prevention of detectable**
444 **infection.** Minimum sample size required per group for specified power to detect a given
445 vaccine efficacy (prevalence in unimmunized mice assumed to be 61.6%).
446
447 **METHODS**
448 **Mice**
449 C57BL/6J mice were purchased from Jackson Laboratories (Bar Harbor, ME). Female mice
450 between the ages of 9-12 weeks were used. All animals were housed and maintained in
451 specific-pathogen-free conditions at Seattle Children's Research Institute (SCRI). All animal
452 studies were performed in compliance with the SCRI Animal Care and Use Committee.
453
454 **BCG Immunizations**
455 BCG-Pasteur was cultured in Middlebrook 7H9 with OADC supplement and 0.05% Tween-80 at
456 37˚C with constant agitation for five days. BCG was back diluted in 7H9 for two days and grown
457 to an OD of 0.2-0.5. Bacteria was diluted in PBS and mice were injected subcutaneously with
458 200µl of 10^6 CFU. After immunization, mice were rested for 8 weeks prior to Mtb infection.
459
460 **ULD Mtb Aerosol Infections**
461 H37Rv or bar-coded H37Rv Mtb were used for infections[11]. Mtb stocks were grown in
462 Middlebrook 7H9 with OADC supplement and 0.05% Tween-80 at 37˚C with constant agitation
463 to an OD = 1. Cultures were filtered through a 5µm filter to remove clumps and aliquots were

464 frozen at -80˚C. Frozen filtered stocks were thawed and titered side by side with stocks used for
465 conventional dose infection to determine how to dilute the ULD stocks with the goal of leaving
466 37% of mice uninfected. Mice were infected using a Glas-Col aerosol infection chamber.
467
468 **CFU Plating**
469 Mouse organs (right lung, left lung, or spleen) were homogenized separately in M tubes
470 containing 1mL PBS+0.05% Tween-80 (PBS-T) using a Miltenyi GentleMACS machine
471 (Miltenyi). Homogenates were then diluted in PBS-T and plated onto 7H10 plates. For ULD
472 infections, undiluted homogenate was also plated between two 7H10 plates. Plates were
473 incubated at 37˚C for at least 21 days before quantification of CFU.
474
475 **Genomic DNA Extraction**
476 Bacterial colonies grown from infected left lungs or right lungs were scraped into resuspension
477 buffer (25mM Tris-HCl pH 7.9, 10mM EDTA, 50mM glucose, water) plus 10mg/mL lysozyme
478 and were incubated at 37˚C overnight. Samples were resuspended in 10% sodium dodecyl
479 sulfate and 10mg/mL Proteinase K and were heated at 55˚C for 30 minutes. Samples were then
480 resuspended in 5M NaCl followed by Cetrimide saline solution and heated at 65˚C for 10
481 minutes. Genomic DNA was extracted twice with 24:1 chloroform:isoamyl alcohol. DNA was
482 precipitated with 0.7x volume of isopropanol and washed with 70% ethanol. Finally, DNA was
483 eluted with DEPC water.
484
485 **Barcoded Sequencing**
486 Mice were infected with a pool of 50 bar-coded strains. Sequencing of bacterial bar-codes has
487 been previously described[11,24]. Briefly, genomic DNA was pre-amplified with pooled barcoded
488 primers before libraries were prepared with NEBNext Ultra DNA Library Prep Kit for Illumina
489 (New England Biolabs) using the AMPure XP reagent (AgenCourt Bioscience) for size selection

490 and cleanup. The NEBNext Multiplex Oligos for Illumina (New England Biosciences) were used
491 to barcode DNA libraries and enabled multiplexing of 96 libraries per sequencing run. Samples
492 were sequenced using the NextSeq 500 Mid Output v2 kit (Illumina) at the University of
493 Washington Northwest Genomics Center. Read alignment was carried out using a custom
494 processing pipeline that has been previously described[24].
495
496 **Statistics**
497 All statistical analysis was done in R v.4.2.0 with packages Exact (v3.1) and lme4 (v1.1-30).
498 When comparing values between two groups in a single experiment, we used Barnard's exact
499 test for differences in proportions and simple linear regression on log-transformed CFU values
500 for differences in bacterial burden. For analyses compiling more than one experiment, we used
501 mixed effects logistic regression with experiment as the grouping variable for differences in
502 proportions, and mixed effects linear regression on log-transformed CFU values for differences
503 in bacterial burden. In all analyses, mice were considered protected when the CFU was
504 undetectable in both lungs, and analyses of dissemination and overall bacterial burden were
505 performed conditional on absence of protection.
506
507 **REFERENCES**
508

509 1. Colditz, G.A., Berkey, C.S., Mosteller, F., Brewer, T.F., Wilson, M.E., Burdick, E., and
510 Fineberg, H.V. (1995). The efficacy of bacillus Calmette-Guerin vaccination of newborns
511 and infants in the prevention of tuberculosis: meta-analyses of the published literature.
512 Pediatrics *96*, 29-35.
513 2. Mangtani, P., Abubakar, I., Ariti, C., Beynon, R., Pimpin, L., Fine, P.E., Rodrigues, L.C.,
514 Smith, P.G., Lipman, M., Whiting, P.F., and Sterne, J.A. (2014). Protection by BCG
515 vaccine against tuberculosis: a systematic review of randomized controlled trials. Clin
516 Infect Dis *58*, 470-480. 10.1093/cid/cit790.
517 3. Abubakar, I., Pimpin, L., Ariti, C., Beynon, R., Mangtani, P., Sterne, J.A., Fine, P.E.,
518 Smith, P.G., Lipman, M., Elliman, D., et al. (2013). Systematic review and meta-analysis
519 of the current evidence on the duration of protection by bacillus Calmette-Guerin

520 vaccination against tuberculosis. Health Technol Assess *17*, 1-372, v-vi.
521 10.3310/hta17370.
522 4. Trauer, J.M., Kawai, A., Coussens, A.K., Datta, M., Williams, B.M., McBryde, E.S., and
523 Ragonnet, R. (2021). Timing of Mycobacterium tuberculosis exposure explains variation
524 in BCG effectiveness: a systematic review and meta-analysis. Thorax *76*, 1131-1141.
525 10.1136/thoraxjnl-2020-216794.
526 5. Schrager, L.K., Vekemens, J., Drager, N., Lewinsohn, D.M., and Olesen, O.F. (2020).
527 The status of tuberculosis vaccine development. Lancet Infect Dis *20*, e28-e37.
528 10.1016/S1473-3099(19)30625-5.
529 6. Karp, C.L., Wilson, C.B., and Stuart, L.M. (2015). Tuberculosis vaccines: barriers and
530 prospects on the quest for a transformative tool. Immunol Rev *264*, 363-381.
531 10.1111/imr.12270.
532 7. Cardona, P.J., and Williams, A. (2017). Experimental animal modelling for TB vaccine
533 development. Int J Infect Dis *56*, 268-273. 10.1016/j.ijid.2017.01.030.
534 8. Lindenstrom, T., Knudsen, N.P., Agger, E.M., and Andersen, P. (2013). Control of
535 chronic mycobacterium tuberculosis infection by CD4 KLRG1- IL-2-secreting central
536 memory cells. J Immunol *190*, 6311-6319. 10.4049/jimmunol.1300248.
537 9. Nemeth, J., Olson, G.S., Rothchild, A.C., Jahn, A.N., Mai, D., Duffy, F.J., Delahaye,
538 J.L., Srivatsan, S., Plumlee, C.R., Urdahl, K.B., et al. (2020). Contained Mycobacterium
539 tuberculosis infection induces concomitant and heterologous protection. PLoS Pathog *16*,
540 e1008655. 10.1371/journal.ppat.1008655.
541 10. Bloom, B.R., and Modlin, R.L. (2016). Mechanisms of Defense against Intracellular
542 Pathogens Mediated by Human Macrophages. Microbiol Spectr *4*.
543 10.1128/microbiolspec.MCHD-0006-2015.
544 11. Plumlee, C.R., Duffy, F.J., Gern, B.H., Delahaye, J.L., Cohen, S.B., Stoltzfus, C.R.,
545 Rustad, T.R., Hansen, S.G., Axthelm, M.K., Picker, L.J., et al. (2021). Ultra-low Dose
546 Aerosol Infection of Mice with Mycobacterium tuberculosis More Closely Models
547 Human Tuberculosis. Cell Host Microbe *29*, 68-82 e65. 10.1016/j.chom.2020.10.003.
548 12. Mollenkopf, H.J., Kursar, M., and Kaufmann, S.H. (2004). Immune response to
549 postprimary tuberculosis in mice: Mycobacterium tuberculosis and Miycobacterium
550 bovis bacille Calmette-Guerin induce equal protection. J Infect Dis *190*, 588-597.
551 10.1086/422394.
552 13. Delahaye, J.L., Gern, B.H., Cohen, S.B., Plumlee, C.R., Shafiani, S., Gerner, M.Y., and
553 Urdahl, K.B. (2019). Cutting Edge: Bacillus Calmette-Guerin-Induced T Cells Shape
554 Mycobacterium tuberculosis Infection before Reducing the Bacterial Burden. J Immunol
555 *203*, 807-812. 10.4049/jimmunol.1900108.
556 14. Bagcchi, S. (2023). WHO's Global Tuberculosis Report 2022. Lancet Microbe *4*, e20.
557 10.1016/S2666-5247(22)00359-7.
558 15. Maglione, P.J., Xu, J., and Chan, J. (2007). B cells moderate inflammatory progression
559 and enhance bacterial containment upon pulmonary challenge with Mycobacterium
560 tuberculosis. J Immunol *178*, 7222-7234. 10.4049/jimmunol.178.11.7222.
561 16. Mayer-Barber, K.D., Andrade, B.B., Barber, D.L., Hieny, S., Feng, C.G., Caspar, P.,
562 Oland, S., Gordon, S., and Sher, A. (2011). Innate and adaptive interferons suppress IL-
563 1alpha and IL-1beta production by distinct pulmonary myeloid subsets during
564 Mycobacterium tuberculosis infection. Immunity *35*, 1023-1034.
565 10.1016/j.immuni.2011.12.002.

566 17. Fine, P.E. (1988). BCG vaccination against tuberculosis and leprosy. Br Med Bull *44*,
567 691-703. 10.1093/oxfordjournals.bmb.a072277.
568 18. Lu, L.L., Smith, M.T., Yu, K.K.Q., Luedemann, C., Suscovich, T.J., Grace, P.S., Cain,
569 A., Yu, W.H., McKitrick, T.R., Lauffenburger, D., et al. (2019). IFN-gamma-
570 independent immune markers of Mycobacterium tuberculosis exposure. Nat Med *25*,
571 977-987. 10.1038/s41591-019-0441-3.
572 19. Behr, M.A., Edelstein, P.H., and Ramakrishnan, L. (2019). Is Mycobacterium
573 tuberculosis infection life long? BMJ *367*, l5770. 10.1136/bmj.l5770.
574 20. Hansen, S.G., Zak, D.E., Xu, G., Ford, J.C., Marshall, E.E., Malouli, D., Gilbride, R.M.,
575 Hughes, C.M., Ventura, A.B., Ainslie, E., et al. (2018). Prevention of tuberculosis in
576 rhesus macaques by a cytomegalovirus-based vaccine. Nat Med *24*, 130-143.
577 10.1038/nm.4473.
578 21. Dijkman, K., Sombroek, C.C., Vervenne, R.A.W., Hofman, S.O., Boot, C., Remarque,
579 E.J., Kocken, C.H.M., Ottenhoff, T.H.M., Kondova, I., Khayum, M.A., et al. (2019).
580 Prevention of tuberculosis infection and disease by local BCG in repeatedly exposed
581 rhesus macaques. Nat Med *25*, 255-262. 10.1038/s41591-018-0319-9.
582 22. Darrah, P.A., Zeppa, J.J., Maiello, P., Hackney, J.A., Wadsworth, M.H., 2nd, Hughes,
583 T.K., Pokkali, S., Swanson, P.A., 2nd, Grant, N.L., Rodgers, M.A., et al. (2020).
584 Prevention of tuberculosis in macaques after intravenous BCG immunization. Nature
585 *577*, 95-102. 10.1038/s41586-019-1817-8.
586 23. Martin, C.J., Cadena, A.M., Leung, V.W., Lin, P.L., Maiello, P., Hicks, N., Chase, M.R.,
587 Flynn, J.L., and Fortune, S.M. (2017). Digitally Barcoding Mycobacterium tuberculosis
588 Reveals In Vivo Infection Dynamics in the Macaque Model of Tuberculosis. mBio *8*.
589 10.1128/mBio.00312-17.
590 24. Ma, S.M., R.; Hobbs, S.J.; Farrow-Johnson, J.; Rustad, T.R.; Sherman, D.R. (2018).
591 Network stress test reveals novel drug potentiators in Mycobacterium tuberculosis.
592 submitted.
593 25. Vidal, S.J., Sellers, D., Yu, J., Wakabayashi, S., Sixsmith, J., Aid, M., Barrett, J.,
594 Stevens, S.F., Liu, X., Li, W., Plumlee, C.R., Urdahl, K.B., Martinot, A.J., Barouch, D.H.
595 (2023). Attenuated Mycobacterium tuberculosis Vaccine Protection in a Low Dose
596 Murine Challenge Model. bioRxiv doi: https://doi.org/10.1101/2023.03.17.533226.

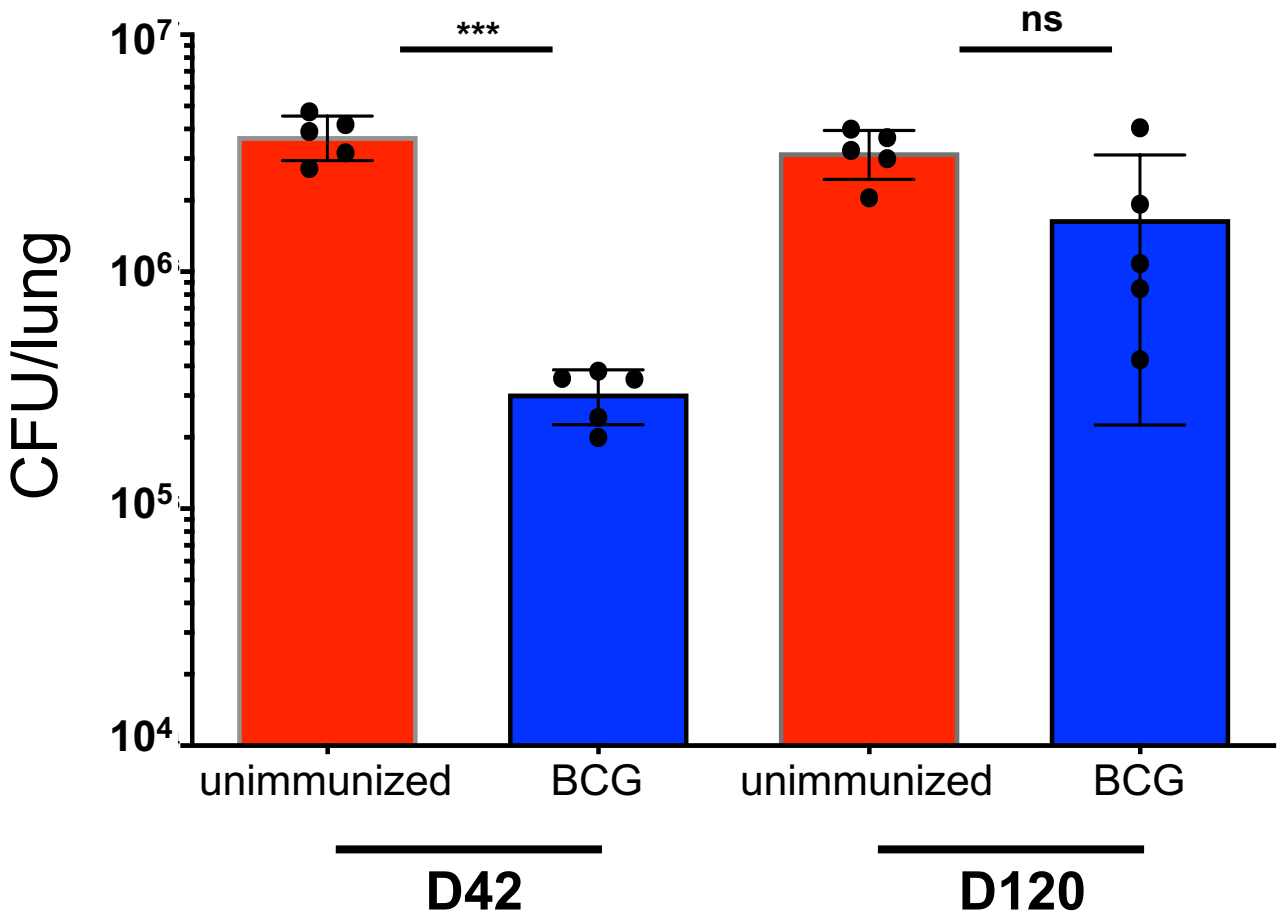
***
ns
10^7
10^6
10^5
10^4
CFU/lung
unimmunized
BCG
unimmunized
BCG
D42
D120

Figure 1

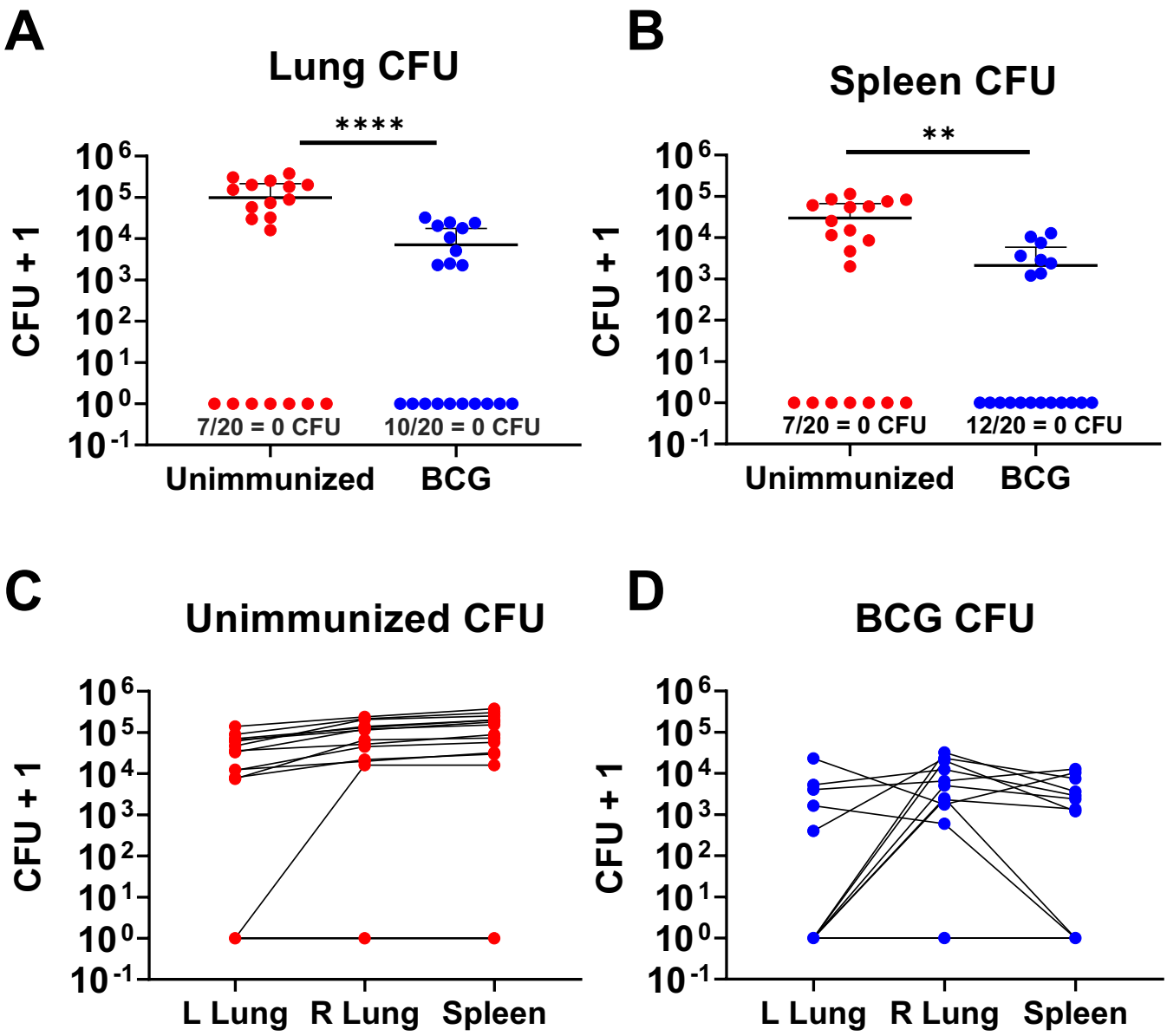
A
Lung CFU
****
CFU + 1
7/20 = 0 CFU
10/20 = 0 CFU
Unimmunized
BCG
B
Spleen CFU
**
CFU + 1
7/20 = 0 CFU
12/20 = 0 CFU
Unimmunized
BCG
C
Unimmunized CFU
CFU + 1
L Lung
R Lung
Spleen
D
BCG CFU
CFU + 1
L Lung
R Lung
Spleen

Figure 2

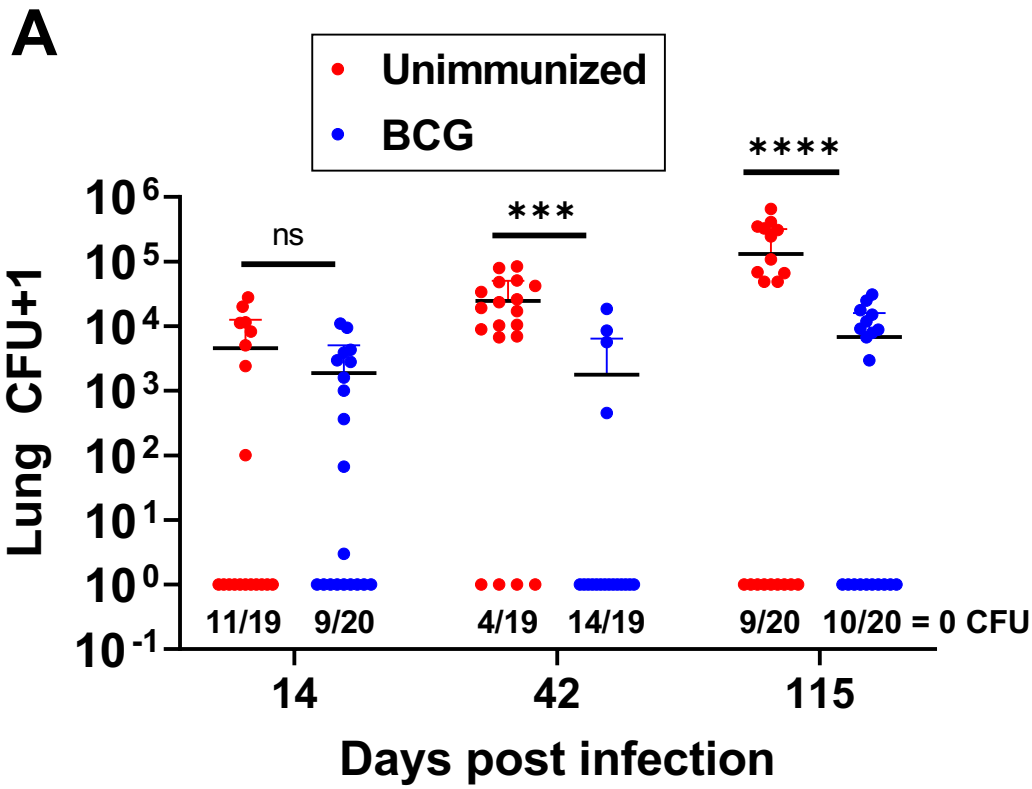
A
Unimmunized
BCG
ns
***
****
Lung CFU+1
10^6
10^5
10^4
10^3
10^2
10^1
10^0
10^{-1}
11/19
9/20
4/19
14/19
9/20
10/20 = 0 CFU
14
42
115
Days post infection

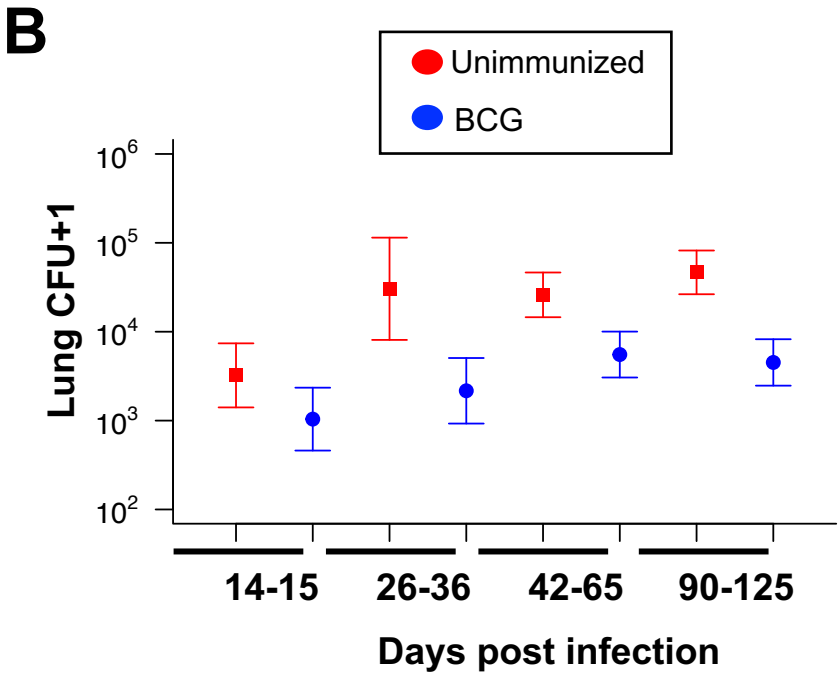
B
Unimmunized
BCG
Lung CFU+1
10^6
10^5
10^4
10^3
10^2
14-15
26-36
42-65
90-125
Days post infection

Figure 3

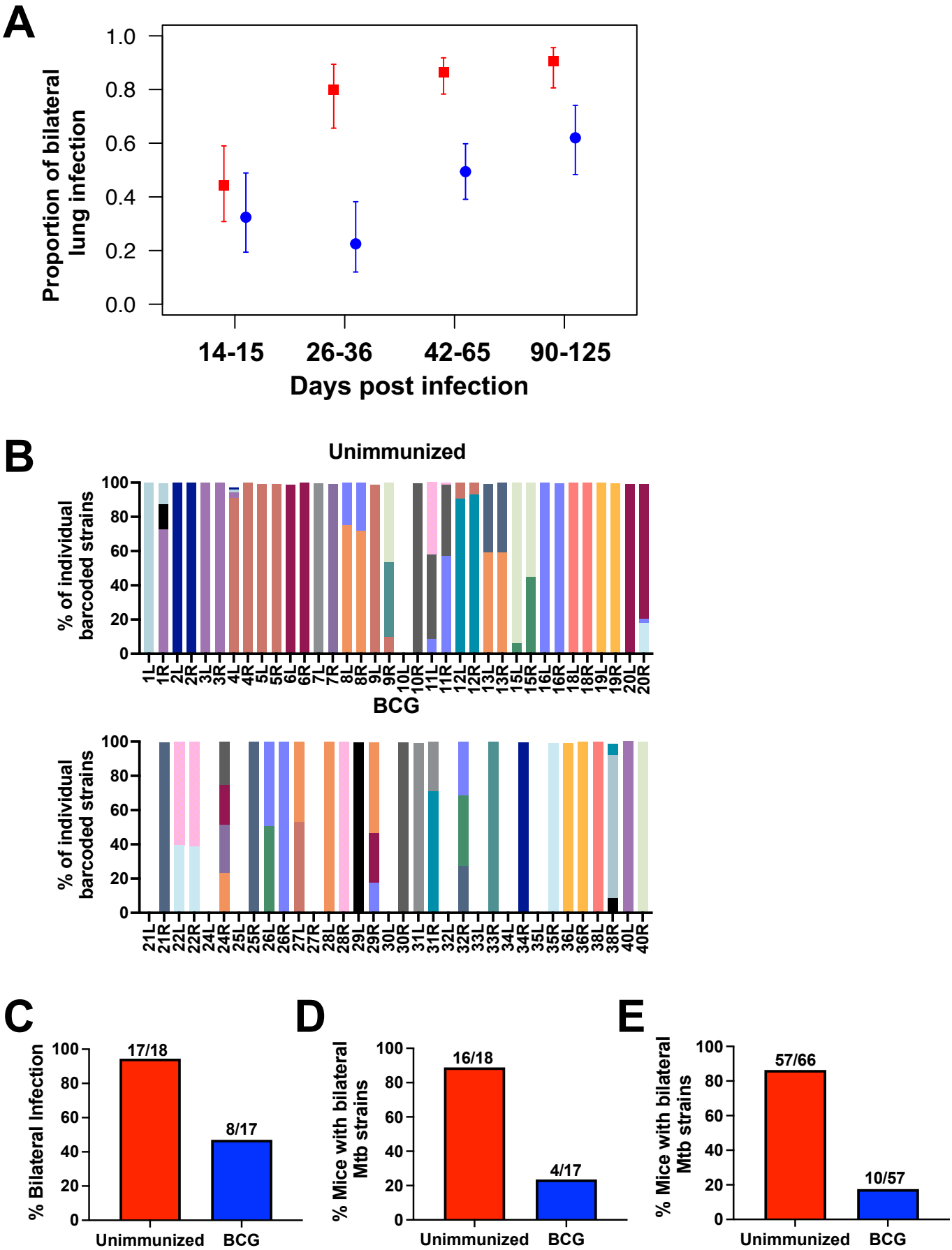
A
Proportion of bilateral lung infection
1.0
0.8
0.6
0.4
0.2
0.0
14-15
26-36
42-65
90-125
Days post infection
B
Unimmunized
% of individual barcoded strains
100
80
60
40
20
0
1L 1R 2L 2R 3L 3R 4L 4R 5L 5R 6L 6R 7L 7R 8L 8R 9L 9R 10L 10R 11L 11R 12L 12R 13L 13R 15L 15R 16L 16R 18L 18R 19L 19R 20L 20R
BCG
% of individual barcoded strains
100
80
60
40
20
0
21L 21R 22L 22R 24L 24R 25L 25R 26L 26R 27L 27R 28L 28R 29L 29R 30L 30R 31L 31R 32L 32R 33L 33R 34L 34R 35L 35R 36L 36R 38L 38R 40L 40R
C
% Bilateral Infection
100
80
60
40
20
0
17/18
8/17
Unimmunized
BCG
D
% Mice with bilateral Mtb strains
100
80
60
40
20
0
16/18
4/17
Unimmunized
BCG
E
% Mice with bilateral Mtb strains
100
80
60
40
20
0
57/66
10/57
Unimmunized
BCG

Figure 4

A

	# mice with undetectable CFU (Unimmunized)	# mice with undetectable CFU (BCG)
All timepoints w/o D14-15	154/440 (35.0%)	191/443 (43.1%)
14-15 dpi	41/97 (42%)	41/100 (41%)
26-36 dpi	34/118 (29%)	40/116 (35%)
42-65 dpi	54/164 (33%)	65/162 (40%)
90-125 dpi	66/158 (42%)	86/165 (52%)

B

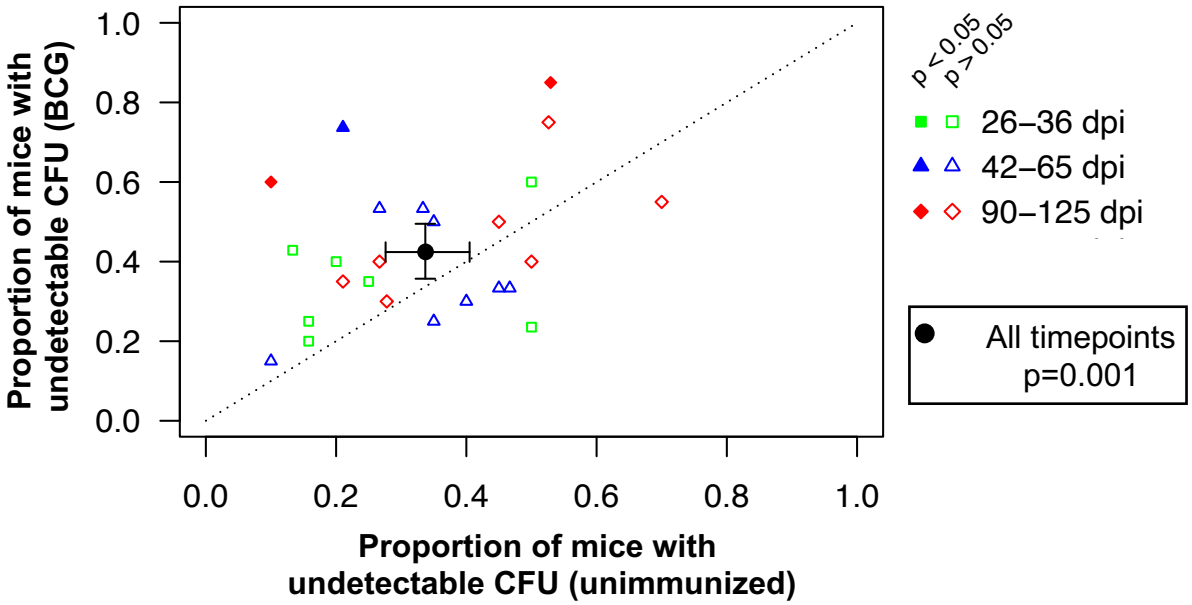

C

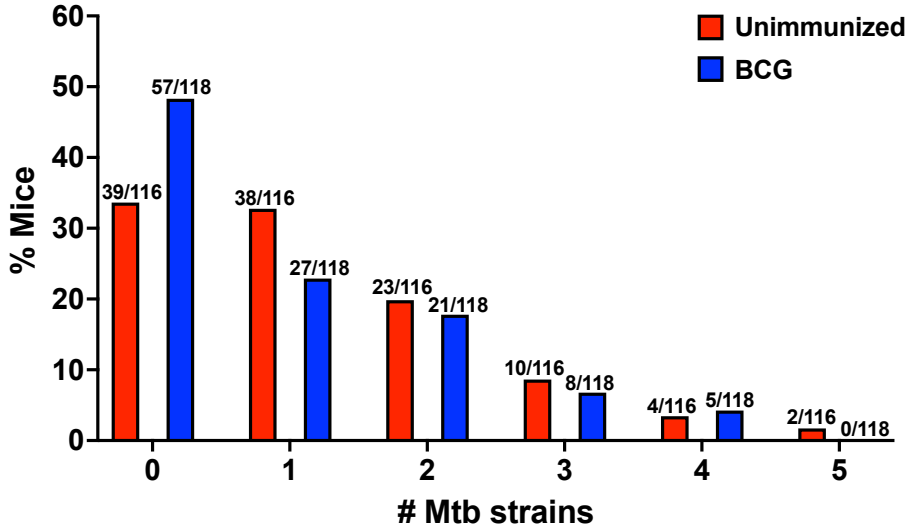

Figure 5

		Min. sample size per group	
Prevalence	**Vaccine efficacy**	**80% Power**	**90% Power**
61.6%	20%	259	342
61.6%	30%	112	155
61.6%	40%	66	84
61.6%	50%	40	55
61.6%	60%	28	37
61.6%	70%	21	25
61.6%	80%	16	18
61.6%	90%	12	16

Table 1